

Gas phase and condensed phase S_Ni reactions. The competitive six and seven centre cyclisations of the 5,6-epoxyhexoxide anion. A joint experimental and *ab initio* study. A comparison with S_Ni reactions of homologous epoxyalkoxide anions †

John M. Hevko, Suresh Dua, John H. Bowie and Mark S. Taylor

Department of Chemistry, The University of Adelaide, South Australia, 5005, Australia

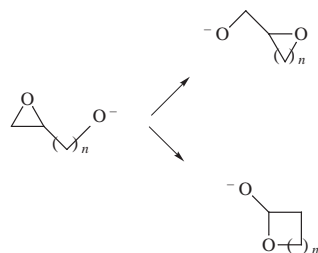
Received (in Cambridge) 12th November 1998, Accepted 22nd December 1998

A. *Ab initio* calculations [at the MP2 Fc/6-31+G(d) level of theory] indicate that the barriers to the transition states for the competitive six and seven centre S_Ni cyclisation processes of the 5,6-epoxyhexoxide anion are 35.0 and 39.7 kJ mol⁻¹ respectively. Experimental studies show that (i) in solution, the 5,6-epoxyhexoxide anion cyclises (and at the same time opens the ethylene oxide ring) to give tetrahydropyran-2-methanol as the predominant product on workup, and (ii) collisional activation of the 5,6-epoxyhexoxide anion in the gas phase gives the 2-tetrahydropyran-methoxide anion as the exclusive anionic product. It is proposed that frequency factors (Arrhenius *A* factors) control the courses of these kinetically controlled gas phase reactions. A comparison of the calculated harmonic vibrational partition functions for the two possible transition states confirms a higher value of Q_{vib} for the reaction proceeding through the six-membered transition state.

B. A comparison is made of the reported competitive S_Ni reactions for 2,3-epoxypropoxide, 3,4-epoxybutoxide, 4,5-epoxypentoxide and 5,6-epoxyhexoxide anions. For all but the 3,4-epoxybutoxide system, the exclusive or major product is that which contains the smaller of the two ring systems for both gas phase and condensed phase reactions. In the case of the 3,4-epoxybutoxide system: (i) in the gas phase, both four and five membered ring S_Ni products are formed in comparable yield, and (ii) in the condensed phase, the major product is that with the larger ring.

Introduction

We have reported the competitive gas phase S_Ni reactions of systems of the type shown in Scheme 1 where $n = 1-3$.¹⁻⁴



Scheme 1

Baldwin's rules⁵⁻⁷ (which refer to stabilised carbanion cyclisations) pertain when $n = 1$ and 3, *i.e.* the predominant cyclisation is that which forms the smaller of the two possible ring systems. The kinetics of these reactions are influenced by the barrier to the transition state and/or the Arrhenius factors *A*.

In this paper we (i) report the behaviour in both the condensed phase and gas phase of the next homologue, *i.e.* where $n = 4$, and (ii) consider all systems so far reported in terms of the parameters influencing the competing cyclisations.

Results and discussion

Part A. The 5,6-epoxyhexoxide system

1. A theoretical approach. There are two major factors which

† Supplementary material is available for this paper (SUPPL. NO. 57479, 9 pp.). For details of the Supplementary Publications Scheme see 'Instructions for Authors', *J. Chem. Soc., Perkin Trans. 2*, available via the RSC web page (<http://www.rsc.org/authors>). The supplementary data are also available on the RSC's web server, <http://www.rsc.org/suppdata/p2/1999/457/>.

determine the relative rates of the two possible cyclisation processes, *viz.* the barriers to the transition state and the Arrhenius (frequency) factor *A*. Both are considered separately below.

a. The results of *ab initio* calculations for competing cyclisations of the 5,6-epoxyhexoxide anion (**1**). The results of an *ab initio* computational study using Gaussian 94⁸ for the system where $n = 4$ are summarised in Fig. 1. The geometries of the local minima and the transition states were optimised at the RHF/6-31+G(d) level of theory, with energies determined at the MP2-Fc/6-31+G(d) level of theory. Energies of **1-3**, **A** and **B** together with the geometries of the two transition states are listed in Table 1. Full geometric data for **1-3** are listed in the Supplementary Data.

The data presented in Fig. 1 and Table 1 show that the barriers to the two transition states **A** and **B** are 35.0 and 39.7 kJ mol⁻¹ at the level of theory indicated. If these modest barriers are controlling the relative rates of the two processes, both **2** and **3** should be formed following collision activation of **1** in the gas phase, with **2** being marginally favoured. Factors which may influence the height of the barriers are as follows. (i) The OCO angles for **A** are 154.42° (dihedral angle 172.93°) and for **B**, 156.38° (dihedral angle 172.25°). These values are very similar: the higher value of 156.38° may, in principle, favour reaction through **B** (*cf.* ref. 7), however any such effect will be marginal. (ii) The larger electrophilicity of the substituted carbon of the ethylene oxide ring (according to Mulliken charge calculations,⁸ C¹ = 0.168 and C² = 0.419) favours nucleophilic attack at the more substituted carbon; *i.e.* formation of **2** through transition state **A**. (iii) The changes in ring strain from **1** to transition states **A** and **B** should be marginal in determining relative kinetics: in contrast, the release in ring strain from **1** to products, makes **2** more thermodynamically stable than **3** [**2** is some 11 kJ mol⁻¹ more negative in energy than product **3** (strain energy of ethylene oxide, tetrahydropyran and oxepan are 112.5, 6.3 and 26.7 kJ mol⁻¹ respectively⁹)].

b. The calculation of Arrhenius factors. Frequency factors for the two competitive S_Ni processes shown in Fig. 1 may be influ-

Table 1 Energies of species shown in Fig. 1, and geometries of transition states **A** and **B**^a

Species	Energies/hartrees (kJ mol ⁻¹)	Geometries/Å or °			
1	-384.4306105 (nominally 0)	<i>b</i>			
2	-384.4678042 (-88.0)	<i>b</i>			
3	-384.4636616 (-76.7)	<i>b</i>			
A	-384.4172435 (+35.0)	C ¹ C ²	1.4450		
		C ² C ³	1.5068		
		C ³ C ⁴	1.5333		
		C ⁴ C ⁵	1.5282		
		C ⁵ C ⁶	1.5356		
		C ⁶ O ⁷	1.3767		
		O ⁷ C ²	2.0844		
		C ² O ⁸	1.7837		
		C ¹ C ² C ³	121.58		
		C ² C ³ C ⁴	113.68		
		C ³ C ⁴ C ⁵	114.10		
		C ⁴ C ⁵ C ⁶	111.37		
		C ⁵ C ⁶ O ⁷	111.62		
		C ⁶ O ⁷ C ²	107.07		
		C ⁷ C ² O ⁸	154.42		
		C ² O ⁸ C ¹	52.09		
		O ⁸ C ¹ C ²	51.02		
		O ⁷ C ² C ¹ O ⁸	172.93		
		B	-384.2565604 (+39.7)	C ¹ C ²	1.4432
				C ² C ³	1.5199
				C ³ C ⁴	1.5326
C ⁴ C ⁵	1.5380				
C ⁵ C ⁶	1.5445				
C ⁶ O ⁷	1.3741				
O ⁷ C ¹	2.0751				
C ¹ O ⁸	1.7467				
O ⁸ C ²	1.4283				
C ¹ C ² C ³	121.05				
C ² C ³ C ⁴	116.54				
C ³ C ⁴ C ⁵	115.34				
C ⁴ C ⁵ C ⁶	117.22				
C ⁵ C ⁶ O ⁷	115.63				
C ⁶ O ⁷ C ¹	104.93				
O ⁷ C ¹ O ⁸	156.38				
C ¹ O ⁸ C ²	52.93				
O ⁸ C ² C ¹	52.15				
O ⁸ C ² C ³	118.18				
O ⁷ C ¹ C ² O ⁸	172.25				

^a Calculations at MP2(fc)/6-31+G(d) level. All energies include zero point energy scaling (factor 0.9676). ^b See Supplementary Data.

enced by (i) the initial nucleophilic attack to form the transition state (*i.e.* the ability of the nucleophile to access the appropriate channel, and the depth of that channel), and/or (ii) the nature of the transition state [*i.e.* whichever is 'looser' (more disordered) will give the higher rate]. To determine the relative abilities of the nucleophile to access the two channels requires an intimate knowledge of the potential surface maps for those processes. We do not have these data. However, the entropic natures of the two transition states may be determined by calculating the relative *A* factors.

To assess the relative Arrhenius *A* factors for the two competing cyclisation channels, we have used transition state theory,¹⁰ *viz.* eqn. (1), where k_B is Boltzman's constant, h is Planck's

$$k(T) = (k_B T/h) (Q^\ddagger/Q_R) \exp(E_0/k_B T) \quad (1)$$

constant, E_0 is the energy difference between reactant and transition state at 0 K, and Q^\ddagger and Q_R are the molecular partition functions of transition state and reactants respectively. The partition function can be factorised into partition functions for translation, rotation, vibration and electronic state,¹⁰ *viz.* eqn. (2).

$$Q = Q_{\text{Trans}} Q_{\text{Rot}} Q_{\text{Vib}} Q_{\text{Elec}} \quad (2)$$

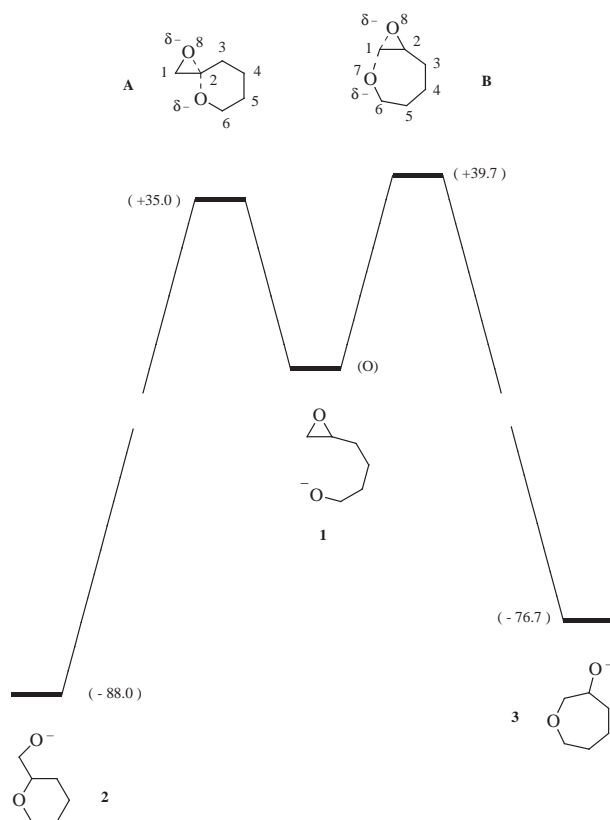


Fig. 1 *Ab initio* calculations at MP2-Fc/6-31G(d) level (Gaussian 94) for the reactions **1**→**2** and **1**→**3**. Energies in kJ mol⁻¹. See Table 1 for the geometries of transition states **A** and **B**. Structures **1**, **2** and **3** have a number of stable conformers. Those shown are the most stable (see Supplementary Data for geometries and energies of the most stable conformers).

Since we are dealing with anions, it seems reasonable to assume that $Q_{\text{Elec}} = 1$. We are dealing with unimolecular rearrangements, so Q_{Trans} of the reactant and transition state are identical, and we assume (to a first approximation) that the same is true for Q_{Rot} . Thus approximation of the *A* factor for each process simplifies to evaluating Q_{Vib} for the reactant and for the competing transition states. However it must be noted that the anions in a mass spectrometer, especially following collisional activation, will not follow a Boltzmann (thermalised) distribution of internal energies. Thus the following calculations must only be considered in a qualitative sense.

We have calculated, at the HF/6-31+G(d) level of theory, the harmonic vibrational frequencies of each structure using Gaussian 94 [*cf.* ref. 11]. These values (scaled by a factor of 0.9131) are listed as Supplementary Data to the paper. A difficulty which often occurs with such an evaluation arises due to the problem of hindered rotors.¹² The calculated vibrational partition functions may underestimate the actual hindered rotor partition functions. Since we are concerned with the ratio of the *A* factors of two competing cyclisation channels which have the same reactant, we have not addressed the hindered rotor problem. The value of Q_{Vib}^\ddagger for the transition state leading to the six-membered ring product (**2**) is 26.3, whereas that for the seven-membered product (**3**) is 63.1, whereas that for the transition state leading to the formation of **2** is 'looser' than that giving **3** (see Supplementary Data for details). The *A* factor for the formation of **2** is thus larger than that for the formation of **3**, within the approximations we have employed.

In summary, (i) *ab initio* calculations indicate that the barriers to the formation of both **2** and **3** from **1** are modest, that both **2** and **3** should be formed under conditions of collision activation, with **2** being the major product. (ii) The relative Arrhenius factors indicate that **A** is the looser transition

Table 2 Reactions of 4,5-epoxyhexanol (**C**), tetrahydropyran-2-methanol (**D**) and 3-oxepanol (**E**) with 10% aqueous sodium hydroxide

Reactant	<i>T</i> /°C	<i>t</i> /h	Product ratio [(C:D:E)%] ^a
C	20	0.16	70:24:6
	20	3	0:72:28
	20	60	0:70:30
	100	0.16	0:61:39
	100	3	0:60:40
	100	60	0:63:37
D	100	60	0:100:0
E	100	60	0:0:100

^a Ratios determined by measuring the areas under each GC peak. Each measurement was carried out twice—error ±2%.

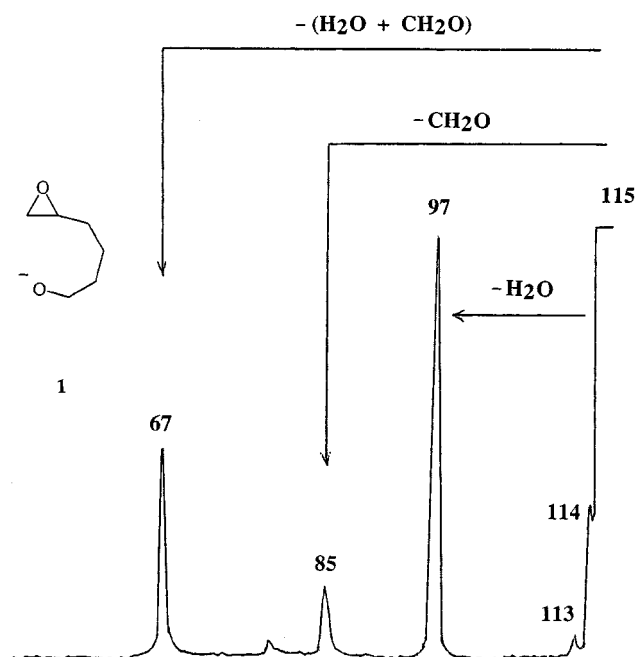


Fig. 2 MS/MS Data for **1**. ZAB 2HF spectrometer. For experimental procedures see Experimental section. Peak widths at half height, *m/z* (volts ± 0.2): 97 (27.4), 85 (33.1) and 67 (30.7).

state by a significant factor. Taken together, these calculations suggest that **2** should be the major cyclisation product in gas phase conditions.

2. The experimental approach. *a. The competitive cyclisation reactions in the condensed phase.* The reactions of 5,6-epoxyhexanol with 10% aqueous sodium hydroxide are summarised in Table 2. Tetrahydropyran-2-methanol is the major product formed at 20 °C, with the product ratio of tetrahydropyran-2-methanol to 3-oxepanol being 65:35 after one hour. The analogous ratio obtained at 100 °C is 60:40. There is no significant change in these product ratios (at constant temperature) with increasing time. Tetrahydropyran-2-methanol and 3-oxepanol are not interconvertible under these conditions, and neither reverts to 5,6-epoxyhexanol. Thus the two competing S_N1 reactions of deprotonated 5,6-epoxyhexanol are kinetically controlled under these reaction conditions.

b. Gas phase cyclisation of the 5,6-epoxyhexoxide anion. Alkoxide ions **1**, **2** and **3** (shown in Fig. 1) were formed in the gas phase by nucleophilic displacement of the appropriate acetate in the ion source of the VG ZAB 2HF mass spectrometer. Forming the alkoxide ions indirectly is necessary, since gas phase deprotonation of the alcohols by HO^- will occur both at OH and elsewhere on these molecules. The collision induced mass spectra of the three alkoxides **1–3** are recorded in Figs. 2–4. Peak widths at half height for the major

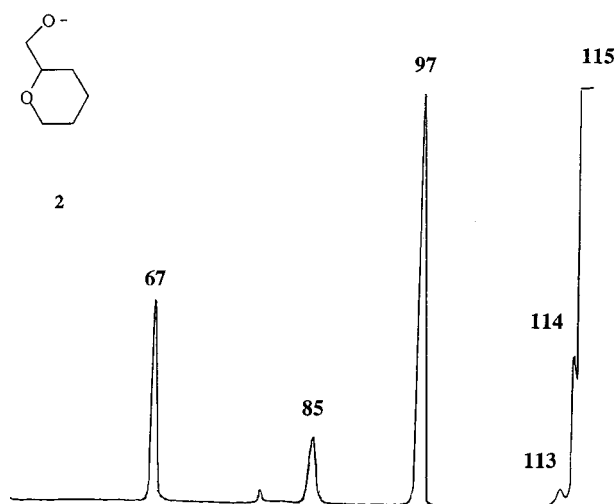


Fig. 3 MS/MS Data for **2**. Peak widths at half height, 97 (27.7), 85 (33.1) and 67 (30.7).

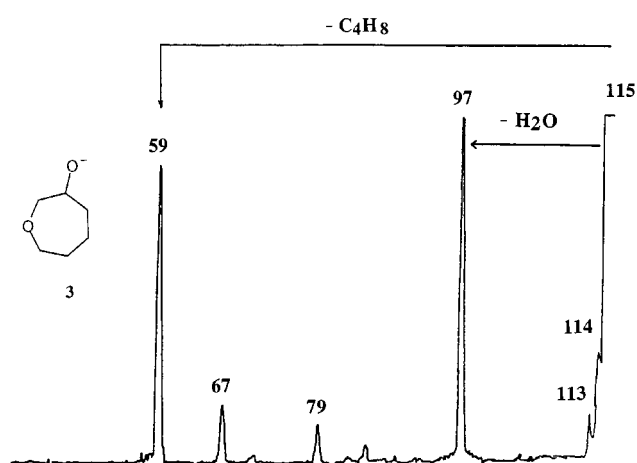


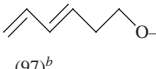
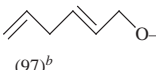
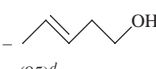
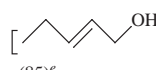
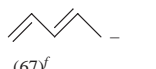

Fig. 4 MS/MS Data for **3**. Width at half height of *m/z* 97 = 33.4 volts.

peaks in these spectra are recorded in the legend to each figure. Data pertaining to product ion studies are listed in Table 3, and the mass spectra of two ^{18}O labelled derivatives are recorded in Table 4.

The spectra of **1** and **2** (Figs. 2 and 3) are the same within experimental error, including identical peak widths at half height of the major peaks *m/z* 97, 85 and 67. These spectra are quite different from that (Fig. 4) of **3**. This indicates that **1** and **2** are fragmenting through a common intermediate (perhaps following cyclisation of **1** to **2**), but that cyclisation of **1** to **3** is not occurring under the reaction conditions. We now need to confirm that (i) the fragment ions from **1** and **2** have the same structures, (ii) there are differences between these structures and those of the fragment anions of **3**, and (iii) fragmentations observed in the spectra of **1** occur following conversion of **1** to **2**.

All data concerning product ion studies are collected in Table 3. Whenever possible, both collisional activation and charge reversal (positive ion)¹³ mass spectra of source formed product anions are compared with those of authentic anions formed by independent syntheses. In some cases, the collisional activation spectra of the fragment ions are either not characteristic (*e.g.* *m/z* 67), or are too weak to make meaningful comparison (*e.g.* *m/z* 59). In these cases, identification is based on the charge reversal spectra. The results of these comparisons are consistent with the data summarised in Scheme 2. The product anions in the spectra of **1** and **2** are the same, but different from those in the spectrum of **3**.

Table 3 Product ion studies using collisional activation (CA) and charge reversal (CR) spectra^a

Parent (<i>m/z</i>)	Product (<i>m/z</i>)	Mode	Spectrum [CA: <i>m/z</i> (loss or formation)abundance] [CR: <i>m/z</i> (abundance)]
1 (115)	-H ₂ O (97)	CA CR	96(H ⁺)100, 95(H ₂)26, 82(CH ₃ ⁺)11, 79(H ₂ O)59, 67(CH ₂ O)68. 97(70), 96(100), 95(78), 81(56), 79(54), 77(34), 69(22), 67(78), 66(44), 65(50), 63(16), 57(4), 55(14), 53(33), 52(34), 51(38), 50(33), 43(8), 41(45), 39(53), 31(6), 29(14), 27(21), 26(16).
2 (115)	-H ₂ O (97)	CA CR	96(H ⁺)100, 95(H ₂)22, 82(CH ₃ ⁺)13, 79(H ₂ O)66, 67(CH ₂ O)70. 97(67), 96(100), 95(75), 81(49), 79(52), 77(38), 69(24), 67(84), 66(47), 65(54), 63(19), 57(4), 55(12), 53(29), 52(30), 51(29), 50(30), 43(6), 41(35), 39(46), 31(3), 29(12), 27(20), 26(15).
3 (115)	-H ₂ O (97)	CA CR	95(H ₂)24, 79(H ₂ O)100, 67(CH ₂ O)1, 41(C ₃ H ₅ ⁻)2. 97(21), 96(76), 95(100), 94(8), 81(52), 79(77), 77(45), 69(18), 67(45), 66(32), 65(28), 63(12), 57(4), 55(8), 53(12), 51(14), 41(21), 39(34), 31(4), 29(8), 27(15), 26(4).
 (97) ^b		CA CR	96(H ⁺)100, 95(H ₂)28, 82(CH ₃ ⁺)5, 79(H ₂ O)65, 67(CH ₂ O)52. 97(68), 96(100), 95(72), 81(52), 79(58), 77(39), 69(21), 67(83), 66(50), 65(55), 63(21), 57(4), 55(12), 53(31), 52(39), 51(32), 50(30), 43(6), 41(37), 39(46), 31(6), 29(12), 27(19), 26(12).
 (97) ^b		CA CR	95(H ₂)24, 79(H ₂ O)100, 67(CH ₂ O)1, 41(C ₃ H ₅ ⁻)1. 97(19), 96(70), 95(100), 94(8), 81(53), 79(66), 77(46), 69(18), 67(39), 66(29), 65(25), 63(11), 57(4), 55(8), 53(13), 51(15), 41(22), 39(37), 31(4), 29(6), 27(11), 26(4).
1 (115)	-CH ₂ O (85)	CA CR	83(H ₂)<20, ^c 67(H ₂ O)60, 55(CH ₂ O)100. 85(4), 84(22), 83(12), 82(5), 81(2), 68(9), 67(60), 66(35), 65(36), 56(28), 55(85), 53(32), 51(26), 50(21), 43(6), 41(42), 39(100), 29(62), 28(16), 27(45), 26(20).
2 (115)	-CH ₂ O (85)	CA CR	83(H ₂)<20, ^c 67(H ₂ O)68, 55(CH ₂ O)100. 85(6), 84(21), 83(13), 82(8), 81(4), 68(14), 67(62), 66(34), 65(38), 56(32), 55(87), 53(33), 51(28), 50(18), 43(8), 41(45), 39(100), 29(65), 28(18), 27(51), 26(20).
 (85) ^d		CA CR	83(H ₂)6, 67(H ₂ O)38, 55(CH ₂ O)100. 85(3), 84(9), 83(12), 82(6), 81(4), 70(5), 69(5), 67(7), 66(6), 65(5), 56(36), 55(100), 54(48), 53(46), 51(22), 50(22), 43(3), 41(24), 39(77), 29(52), 28(28), 27(42), 26(16).
 (85) ^e		CA CR	67(H ₂ O)100, 55(CH ₂ O)1. 85(3), 84(83), 83(97), 82(5), 81(2), 70(1), 69(2), 68(15), 67(17), 66(10), 65(10), 57(2), 56(8), 55(29), 53(12), 51(9), 50(10), 43(6), 41(43), 39(100), 29(76), 28(26), 27(64), 26(18).
1 (115)	-(H ₂ O + CH ₂ O) (67)	CR	67(100), 66(48), 65(34), 64(3), 63(6), 62(3), 61(2), 53(1), 52(4), 51(6), 50(5), 49(2), 41(7), 40(3), 39(10), 38(2), 37(1), 27(2), 26(1).
2 (115)	-(H ₂ O + CH ₂ O) (67)	CR	67(100), 66(50), 65(35), 64(2), 63(7), 62(3), 61(2), 53(1), 52(4), 51(6), 50(5), 49(2), 41(7), 40(2), 39(8), 38(2), 37(1), 27(2), 26(1).
 (67) ^f		CR	67(100), 66(54), 65(36), 64(2), 63(7), 62(3), 61(2), 53(1), 52(4), 51(4), 50(3), 49(1), 41(6), 40(2), 39(7), 38(2), 37(1), 27(2), 26(1).
 (67) ^g		CR	67(100), 66(51), 65(39), 64(2), 63(7), 62(2), 61(1), 53(1), 52(5), 51(8), 50(7), 49(2), 41(22), 40(10), 39(39), 38(7), 37(4), 27(8), 26(3).
3 (115)	-C ₄ H ₈ (59)	CR	59(8), 58(29), 57(6), 56(8), 45(2), 44(4), 42(13), 41(15), 31(34), 30(48), 29(100), 28(32).
-OCH ₂ CHO (59) ^h		CR	59(10), 58(28), 57(4), 56(12), 45(2), 44(6), 42(18), 41(19), 31(29), 30(43), 29(100), 28(34).

^a The abundances in both collisional activation and charge reversal spectra are dependent on both source conditions and the collision gas pressure. As a general guide when comparing spectra, the abundance of an individual peak should be correct to $\pm 10\%$. ^b Formed by deprotonation of the appropriate alcohol with HO⁻. ^c Weak spectrum: difficult to measure the abundance of the peak formed by loss of H₂ because of baseline noise. ^d Formed by decarboxylation of HOCH₂CH₂CH=CHCH₂CO₂⁻. ^e Formed by deprotonation of MeCH₂CH=CHCH₂OH with HO⁻. ^f Formed by deprotonation of penta-1,3-diene with HO⁻. ^g Formed by deprotonation of cyclopentene with HO⁻. ^h Reported by spectrum, see ref. 3.

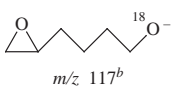
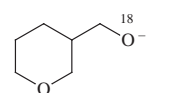
The data considered to date show that **1** and **2** have identical fragmentations but do not indicate whether **1** cyclises to **2** before fragmentation occurs. This problem is resolved from a consideration of the spectra (Table 4) of ¹⁸O labelled derivatives (of **1** and **2**). These spectra demonstrate the equilibration of the two oxygens of **1** (and **2**) prior to fragmentation: in the case of **1**, such equilibration requires rearrangement of **1** to **2** prior to fragmentation. The fragmentations of **2** have been considered previously: it has been proposed that the oxygen equilibration occurs by the proton transfer/ring opening equilibria summarised in Scheme 3.¹⁴ Fragmentation of the ring opened structures, particularly **4/5** and **6/7**, account for both the oxygen equilibration and the structures of the product ions (Scheme 2) formed by the respective losses of H₂O and CH₂O.

We have not carried out labelling studies on the 3-oxepanol anion **3**: our primary interest in **3** was to determine whether its fragmentations are different from those of **1** and **2**. Even so, the formation of *m/z* 59 (Scheme 2) is straightforward, while the structure of *m/z* 97 is consistent with the fragmentation pathway shown in Scheme 4.

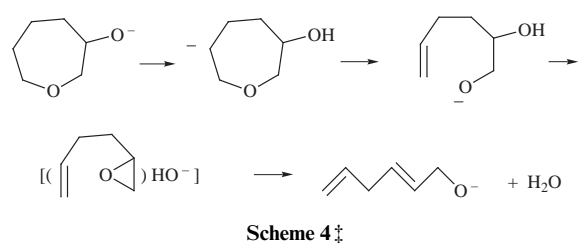
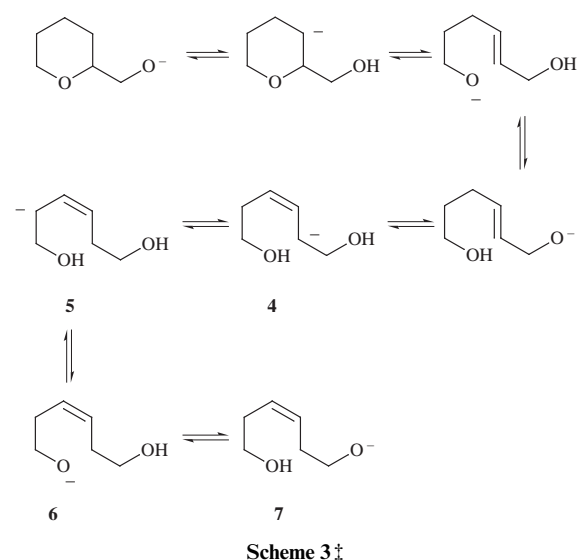
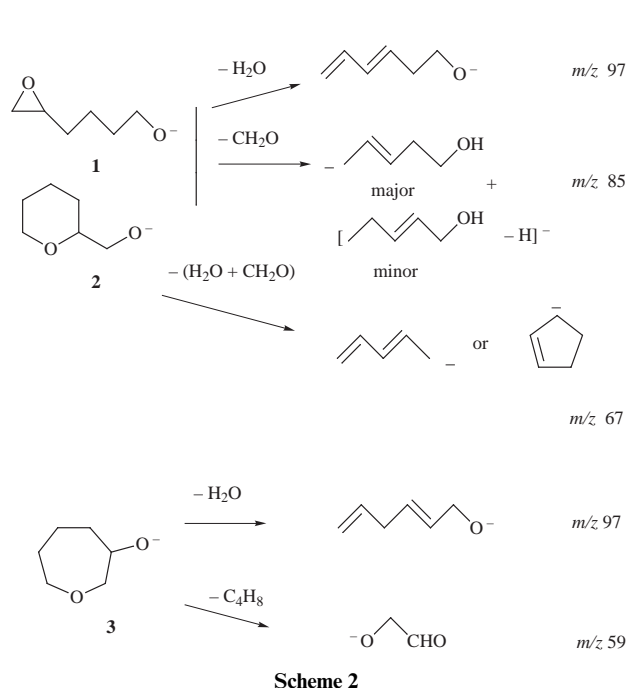
Conclusions to Part A. 1. *Ab initio* and Arrhenius factor calculations indicate that **1** should cyclise to both **2** and **3**. The barriers to transition states **A** and **B** are modest (computed as 35.0 and 39.7 kJ mol⁻¹ respectively), and the Arrhenius factor is larger for the formation of **2** than for **3**. Thus **2** is predicted to be the favoured product.

2. Experimentally, **1** cyclises to give only **2** in the gas phase: product **3** is not detected. It is proposed that the larger

Table 4 CA MS/MS Data for ^{18}O labelled **1** and **2**

Parent	Spectrum [m/z (loss or formation)relative abundance]
 m/z 117 ^b	116/115 ^a (H ⁺ , H ₂)20, 99(H ₂ O)100, 97(H ₂ ¹⁸ O)85, 87(CH ₂ O)8, 85(CH ₂ ¹⁸ O)10, 79(H ₂ O + H ₂ ¹⁸ O)5, 67(C ₅ H ₇ ⁻)47.
 m/z 117 ^{b,c}	116(H ⁺)24, 115(H ₂)5, 99(H ₂ O)64, 97(H ₂ ¹⁸ O)70, 87(CH ₂ O)17, 85(CH ₂ ¹⁸ O)14, 79(H ₂ O + H ₂ ¹⁸ O)8, 67(C ₅ H ₇ ⁻)100.

^a Unresolved peaks. ^b The ^{18}O label is in the side chain of **1**: cyclisation of **1** will give **2** with the ^{18}O label in the ring. Thus the relative ratios of m/z 99:97 and 87:85 will be reversed in the two spectra, as observed. ^c The relative abundances of the major fragment peaks in the spectra of **1** and **2** are critically dependent on collision gas pressure. This explains the major abundance differences in the two spectra above (*cf. e.g. m/z* 67) (the two spectra were measured six years apart, see ref. 14): this does not affect the 99:97 and 87:85 ratios.



Arrhenius factor for reaction **1** to **2** is a major contributing factor to the exclusivity of this reaction (*i.e.* entropically, transition state **A** is 'looser' than transition state **B**).

3. Treatment of **1** in 10% aqueous sodium hydroxide at reflux yields both **2** and **3** in kinetically controlled reactions, with **2** being the predominant product.

Part B. Comparison of the competing reactions of Scheme 1 where $n = 1-4$.

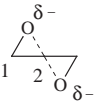
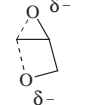
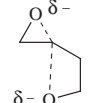
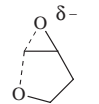
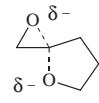
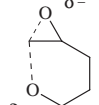
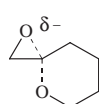
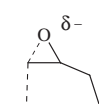
We now summarise the results for the four homologous systems for which competing S_Ni processes have been studied in the gas phase.¹⁻⁴ A number of parameters which influence the formation of the eight transition states of the four systems ($n = 1$ to 4; *cf.* Scheme 1) are listed in Table 5. These kinetic parameters are calculated for gas phase reactions, *i.e.* for reactions occurring in the absence of solvent. The transition states are numbered as follows: **1.1** ($n = 1$)—the Payne rearrangement, S_Ni through three centre state, **1.2** ($n = 1$)— S_Ni through the competing four membered transition state; **2.1** ($n = 2$)— S_Ni through four centre state, **2.2** ($n = 2$)— S_Ni through the competing five centred state, *etc.* The parameters listed are (i) the O-C-O angle for the S_Ni process at the transition state, together with the corresponding dihedral angle, (ii) the computed barrier from reactant to the transition state (in kJ mol^{-1}), (iii) the Mulliken charge ratio (the relative electrophilicities) of

C¹ and C² (the two carbons on the ethylene oxide ring) of the reactant, and (iv) the Arrhenius factor (Q_{vib}) for each reaction (determined as outlined in Part A). The bond lengths of the breaking and forming bonds in the various transition states are not listed because they are comparable for all systems (except for symmetrical **1.1** where the O-C bonds are both 1.89 \AA), *i.e.* the forming bonds are longer (in the range $2.08-2.10 \text{ \AA}$) than the breaking bonds (within the range $1.74-1.89 \text{ \AA}$).²⁻⁴ The major (and minor) products obtained both in the gas and condensed phases from each pair of transition states are also listed in Table 5.

Three of the four systems show significant correspondence between the experimental gas phase (and condensed phase) data and the theoretical data ($n = 1, 3$ and 4), while one ($n = 2$) shows some deviation. When $n = 1$, the Payne rearrangement is the major process in the gas phase: a feature in accord with *ab*

‡ The second structure may be transient or alternatively the formation of the third structure from the first may be concerted. The second structure is included in the Scheme in order that the mechanism for ring opening is clear.

Table 5 Parameters influencing the kinetics of competitive S_N2 processes. Major products

Transition state	Barrier/kJ mol ⁻¹ ^a	O–C–O (dihedral) ^o	Mulliken C ¹ :C ² ^b	Arrhenius Q_{vib} ^c	Product(s)		
					Gas phase	Condensed phase ^d	
	1.1	45 ^e	160.1 (159.7)	0.189:0.349	3.4	Major	^f
	1.2	122 ^e	116.5 (153.0)		2.5	Minor	
	2.1	70	163.4 (163.1)	0.158:0.336	9.8	Major ^g	Minor
	2.2	69	140.4 (163.1)		4.7	Major ^g	Major
	3.1	48	156.1 (176.1)	0.181:0.329	20.5	Sole product	Major
	3.2	48	152.8 (175.3)		10.2	—	Minor
	4.1	35	154.4 (172.9)	0.168:0.419	63.1	Sole product	Major
	4.2	40	156.4 (172.3)		26.3	—	Minor

^a At MP2-Fc/6-31+G(d) level. ^b The Mulliken charge distribution is that of C¹ and C² in the reactant, see ref. 8. ^c Calculations as described earlier in this paper. ^d Carried out in 10% aqueous sodium hydroxide at reflux (for full details see refs. 2–4). ^e Calculations at G2 level in these two cases. ^f Not performed. However alkyl substituted 2,3-epoxypropoxide anions exclusively undergo the Payne rearrangement in solution, *cf.* ref. 1. ^g Gas phase experiments only indicate that both are formed in approximately comparable yield, see ref. 3.

initio data. The Payne rearrangement (which proceeds through transition state **1.1**) is favoured by the lower barrier of 45 kJ mol⁻¹ (*cf.* 122 kJ mol⁻¹ for **1.2**). The major contributor to the larger barrier to transition state **1.2** is the unfavourable geometry of the transition state, *i.e.* angle O–C–O is computed to be 116.5° (*cf.* 160.1° for **1.1**: the closer the O–C–O angle is to the ideal S_N2 angle of 180°, the more favoured will be the reaction if other parameters are equal). Although the larger Arrhenius factor also favours the formation of transition state **1.1**, the large barrier difference is a major factor influencing the competing S_N2 reactions when $n = 1$.

The gas phase results for systems where $n = 3$ and 4 are perhaps surprising but they are consistent and qualitatively similar to the predictions of the *ab initio* studies. The computed barriers for each of the competing reactions when $n = 3$ and 4 are comparable in each system (48 kJ mol⁻¹ for **3.1** and **3.2**; 35 and 40 kJ mol⁻¹ for **4.1** and **4.2**), yet in both cases there is only one product formed in the gas phase, *viz.* those formed through

3.1 and **4.1** respectively. The Arrhenius factor must control the gas phase reaction when $n = 3$. The same scenario probably also pertains when $n = 4$. Although the barriers are different (35 and 40 kJ mol⁻¹), they are very modest, and if they are a major influence in determining the product ratio, then products should be observed from both processes. We propose that frequency factors are controlling the gas phase S_N2 reactions where $n = 3$ and 4. The condensed phase reactions (in 10% aqueous sodium hydroxide at reflux) show the expected trend. The smaller of the ring systems is formed predominantly in each case.

The situation with regard to the system when $n = 2$ is not as clear as those of the three systems described above. The potential profile summarising the *ab initio* calculations³ is recorded in Fig. 5 to assist the discussion. This system shows similarities to that where $n = 3$, *i.e.* the barriers to the two processes are comparable (see Fig. 5 and *cf.* Table 5) as are the Mulliken and the Arrhenius Q_{vib} ratios (see Table 5).

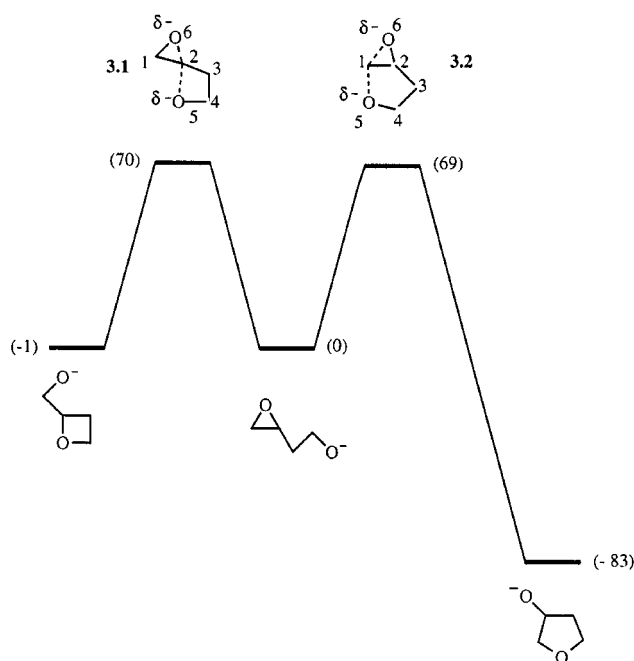


Fig. 5 *Ab initio* calculations [geometries RHF/6-31+G(d), energies MP2-Fc/6-31+G(d)] for competitive S_Ni cyclisations of the 3,4-epoxybutoxide anion (from ref. 4).

There is however one feature which distinguishes this system from the other three, *viz.*, the two product alkoxides have very different thermodynamic stabilities. The five membered ring product is 82 kJ mol⁻¹ more negative in energy than the four membered counterpart (see Fig. 5) [*cf.* -27 ($n=1$, *i.e.* oxetane product more stable than ethylene oxide product),¹ -26 ($n=3$)⁴ and +11 kJ mol⁻¹ ($n=4$, see Fig. 1 this paper)]. This large difference of 82 kJ mol⁻¹ is due principally to the difference in ring strain between the oxetane and tetrahydrofuran systems (107.5 and 25.1 kJ mol⁻¹ respectively⁹).

The system depicted in Fig. 5 is the most complex we have studied from an experimental viewpoint. Consideration of the spectra of the three alkoxide anions shown in Fig. 5 together with those of ²H and ¹⁸O labelled derivatives, show that in the gas phase, (i) both cyclisation products are formed in comparable yield, (ii) the three and four membered systems are interconvertible under conditions of collisional activation, and (iii) the tetrahydrofuran methoxide product does not interconvert to the reactant. It is possible that thermodynamic control explains the formation of at least some of the tetrahydrofuran methoxide product: the exothermicity of this process and the consequent high reverse energy barrier are in keeping with such a proposal.

This system has also been studied in two different solvent systems, *i.e.* 10% aqueous sodium hydroxide and sodium hydride/tetrahydrofuran, both at reflux. The products were identified using gas chromatography/mass spectrometry with a Finnigan GCQ ion trap mass spectrometer.³ The experimental results (which are reproducible) show that tetrahydrofuran-methanol is the major product in both solvent systems. We anticipated that this result should be explicable in terms of the reactions being thermodynamically controlled in solution. However this appears not to be the case: tetrahydrofuran-methanol is the kinetic product as evidenced by the product ratios being the same (within experimental error) at reaction times within the range 10 min to 60 h.³

Conclusions to Part B. For the scenario outlined in Scheme 1: (i) The gas phase S_Ni reactions for the systems ($n=1, 3$ and 4) give the smaller ring system either exclusively or in the larger yield. This is in accord with the theoretical studies and with

Baldwin's rules.⁵⁻⁷ When $n=2$, both products are formed in comparable yield.

(ii) The corresponding condensed phase reactions preferentially give the smaller ring system in higher yield when $n=1, 3$ and 4. When $n=2$, the larger ring system is formed in the higher yield.

Experimental

Mass spectrometric methods

Collisional activation (CA) mass spectra (MS/MS) were determined with a VG ZAB 2HF mass spectrometer.¹⁵ Full operating details have been reported.¹⁶ Specific details were as follows: the chemical ionisation slit was used in the chemical ionisation source, the ionising energy was 70 eV, the ion source temperature was 100 °C, and the accelerating voltage was 7 kV. The liquid samples were introduced through the septum inlet with no heating [measured pressure of sample 1×10^{-6} Torr (1 Torr = 133.322 Pa)]. Alkoxide anions 1-3 were formed by S_N2 displacement from the appropriate acetate using HO⁻ (from H₂O: measured pressure 1×10^{-5} Torr). The estimated source pressure was 10⁻¹ Torr. Argon was used in the second collision cell (measured pressure, outside the cell, 2×10^{-7} Torr), giving a 10% reduction in the main beam, equivalent to single collision conditions. CID MS/MS measurements involved using the magnet to choose the ion under study, collision activating it (see above), and scanning the electric sector to analyse the resultant product anions. Charge reversal (CR) (positive ion) MS/MS data for negative ions were obtained as for CA MS/MS data, except that the electric sector potential was reversed to allow the transmission of positively charged product ions (for full details see ref. 13). The recorded peak widths at half height are an average of ten individual measurements and are correct to ± 0.2 volts.

Ab initio calculations

The Gaussian 94⁸ suite of programs was used for all calculations, which were carried out on Silicon Graphics Power Challenge. The geometries of the local minima and the transition states were optimised at the RHF/6-31+G(d) and MP2 (Fc)/6-31+G(d,p) levels of theory. Harmonic frequency analyses were performed on each stationary point in order to characterise them as either a local minimum or transition state. A local minimum is characterised by possessing all real vibrational frequencies and its hessian matrix possessing all positive eigenvalues. A transition state is characterised by possessing one (and only one) imaginary frequency and its hessian matrix possessing one (and only one) negative eigenvalue. Intrinsic reaction coordinate (IRC) calculations were performed (beginning from both transition structures) to verify that each transition structure connected particular local minima. Final energies are quoted at the MP2 Fc/6-31+G(d) level of theory, and include a scaled (0.8929) zero point vibrational energy correction [which is based on the RHF/6-31+G(d) optimised geometry].

Materials

Tetrahydropyran-2-methanol, penta-1,3-diene and pent-4-en-1-ol were commercial samples. Tetrahydropyran-2-methanol acetate,¹⁷ 5,6-epoxyhexanol,¹⁸ 5,6-epoxyhexyl acetate,¹⁹ 3-oxepanol,¹⁹ hexa-3,5-diene-1-ol,²⁰ and hexa-2,5-dien-1-ol²¹ were made by reported procedures.

3-Acetoxyoxepan. 3-Oxepanol (0.1 g) was acetylated by a standard procedure¹⁷ to yield 3-acetoxyoxepane (bp 121–123 °C/760 mmHg; 0.11 g, 81% yield). Found, C, 60.6; H, 9.2%: C₈H₁₄O₃ requires C, 60.7; H, 8.9%. MH⁺ = 159 (18%), base peak *m/z* 43. ¹H NMR (300 MHz, CDCl₃) δ 1.35–1.52 (4H, m), 1.70–1.82 (2H, q), 2.01 (3H, s), 3.4 (2H, d), 3.69 (2H, t), 4.1

(1H, m). ¹³C NMR (CDCl₃) δ 21.1 (CH₃), 21.39 (CH₂), 27.5 (CH₂), 31.82 (CH₂), 64.1 (CH), 70.4 (CH₂), 170.5 (C=O).

[1-¹⁸O]5,6-Epoxyhexan-1-ol. Hex-5-en-1-ol (2 g) was oxidised²² to hex-5-enoic acid (1.9 g, 83%), which was stirred at 20 °C with oxalyl chloride (1.5 cm³) and *N,N*-dimethylformamide (1 drop) in anhydrous diethyl ether (30 cm³) for 3 h. Removal of the solvent *in vacuo* followed by distillation gave hex-5-enoyl chloride (1.4 g, 73%), which was allowed to stir with H₂¹⁸O (0.26 g, 96% ¹⁸O) and tetrahydrofuran (10 cm³). The solution was dried (MgSO₄) and concentrated under reduced pressure to afford a clear oil which was added dropwise to a suspension of lithium aluminium hydride (0.5 g) in diethyl ether (20 cm³) and heated at reflux for 2 h. The mixture was cooled to 0 °C, aqueous hydrogen chloride (30%, 2 cm³) was added, the organic layer separated, the aqueous layer extracted with diethyl ether (2 × 5 cm³), the combined organic extracts dried (MgSO₄), concentrated *in vacuo*, and the residue distilled to give [1-¹⁸O]hex-5-en-1-ol (0.75 g), which was epoxidised¹⁸ and distilled (60–70 °C/20 mmHg) to afford the ¹⁸O labelled alcohol (0.5 g, 58% yield; ¹⁸O = 48%).

The corresponding acetate was made by a standard technique.¹⁹

Condensed phase reactions

Products of the base catalysed reactions of 5,6-epoxyhexanol, tetrahydropyran-2-methanol and 3-oxepanol were analysed using a Finnigan GCQ mass spectrometer. Conditions: Column phase RTX-SMS (length 30 cm, ID 0.25, GC fused silica capillary), He carrier gas. Initial column temperature, held at 50 °C for 2 min, then the temperature increases at 15 °C per min. Retention times: 5,6-epoxyhexanol (7.00 min), tetrahydropyran-2-methanol (6.02 min) and 3-oxepanol (6.32 min).

A mixture of 5,6-epoxyhexanol (0.5 g) and aqueous sodium hydroxide (10%, 5 cm³) was allowed to stir for 60 h, (i) at 20 °C, and (ii) at 100 °C (see Table 2). The reaction mixtures were sampled at various times. Each sample was acidified with aqueous hydrogen chloride (10%) until the pH was 6, extracted with dichloromethane (5 cm³), the organic extract dried (MgSO₄) and concentrated. The product composition was analysed by GC/MS (see Table 2).

Tetrahydropyran-2-methanol and 3-oxepanol were each treated with aqueous sodium hydroxide as detailed above. No reaction was observed in either case.

Acknowledgements

This research was financed by the Australian Research Council.

J. M. H., M. S. T and S. D. thank the ARC for a PhD scholarship, a research associate position and a research assistant position respectively.

References

- 1 S. Dua, M. S. Taylor, M. A. Buntine and J. H. Bowie, *J. Chem. Soc., Perkin Trans. 2*, 1997, 1991.
- 2 S. Dua, M. S. Taylor, M. A. Buntine and J. H. Bowie, *Int. J. Mass Spectrom. Ion Processes*, 1997, **165/166**, 139.
- 3 J. M. Hevko, S. Dua, J. H. Bowie and M. S. Taylor, *J. Chem. Soc., Perkin Trans. 2*, 1998, 1629.
- 4 J. M. Hevko, S. Dua, M. S. Taylor and J. H. Bowie, *Int. J. Mass Spectrom.*, 1998, in the press.
- 5 L. Tenud, S. Farook, J. Seibl and A. Eshenmoser, *Helv. Chim. Acta*, 1970, **53**, 2059.
- 6 G. Stork and J. F. Cohen, *J. Am. Chem. Soc.*, 1974, **96**, 5270.
- 7 J. E. Baldwin, *J. Chem. Soc., Chem. Commun.*, 1976, 734; J. E. Baldwin, *Further Perspectives in Organic Chemistry*, A Ciba Foundation Symposium, Elsevier, Amsterdam, 1978, 85.
- 8 GAUSSIAN 94, Revision C3, M. J. Frisch, G. W. Trucks, H. B. Schlegel, P. M. W. Gill, B. G. Johnson, M. A. Robb, J. R. Cheeseman, T. Keith, G. A. Petersson, J. A. Montgomery, J. B. Foresman, J. Cioslowski, B. B. Stefanov, A. Nanayakkara, M. Challacombe, C. Y. Peng, P. V. Ayala, W. Chen, M. W. Wong, J. L. Andres, E. S. Replogle, R. Gomperts, R. L. Martin, D. J. Fox, J. S. Binkley, D. J. Defrees, J. Baker, J. P. Stewart, M. Head-Gordon, C. Gonzales and J. A. Pople, Gaussian Inc., Pittsburgh, PA, 1995.
- 9 S. W. Benson, *Thermochemical Kinetics*, Wiley, New York, 1967.
- 10 R. G. Gilbert and S. C. Smith, *Theory of Unimolecular and Recombination Reactions*, Blackwell Scientific, Cambridge, 1990.
- 11 A. P. Scott and L. Radom, *J. Phys. Chem.*, 1996, **100**, 16502.
- 12 J. P. A. Heuts, R. G. Gilbert and L. Radom, *Macromolecules*, 1995, **28**, 8771.
- 13 J. H. Bowie and T. Blumenthal, *J. Am. Chem. Soc.*, 1975, **97**, 2959; I. Howe, J. H. Bowie, J. E. Szulejko and J. H. Beynon, *Int. J. Mass Spectrom. Ion Processes*, 1980, **34**, 99.
- 14 S. Dua, R. A. J. O'Hair, J. H. Bowie and R. N. Hayes, *J. Chem. Soc., Perkin Trans. 2*, 1992, 1151.
- 15 VG ZAB 2HF, VG Analytical, Manchester, UK.
- 16 M. B. Stringer, J. L. Holmes and J. H. Bowie, *J. Am. Chem. Soc.*, 1986, **108**, 3888.
- 17 T. Shono, Y. Matsumua, O. Onomura and Y. Yamada, *Synthesis*, 1987, **12**, 1099.
- 18 K. Nishitani, Y. Harada, Y. Nakamura, K. Yokoo and Y. Yamakawa, *Tetrahedron Lett.*, 1994, **35**, 7809.
- 19 M. Mihailovic and D. Marinkovic, *Croatica Chem. Acta*, 1986, **59**, 109.
- 20 S. Martin, C. Tu and T. Chou, *J. Am. Chem. Soc.*, 1980, **102**, 5274.
- 21 J. Appo Rao and M. P. Cava, *J. Org. Chem.*, 1989, **54**, 2751.
- 22 E. J. Eisenbraun, *Org. Syn. Coll. Vol. 5*, 1973, 5274.